

# Top quark property measurements with the CMS experiment

**O. Hindrichs**

On behalf of the CMS collaboration

University of Rochester

**BLOIS 2024**

Oct 24, 2024

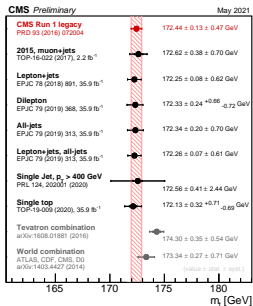
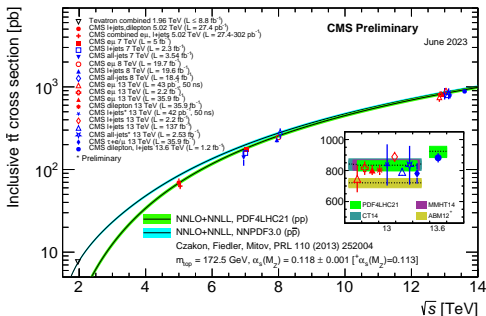


UNIVERSITY of  
ROCHESTER



# Introduction

Cross sections of 830 pb (920 pb) at 13 TeV (13.6 TeV)  $\rightarrow$  about 100M  $t\bar{t}$  pairs in Run 2



- Status and conclusions from (multi) differential cross sections measurements
- News from measurements of spin correlations and observation of entanglement
- New techniques for  $m_t$  measurements

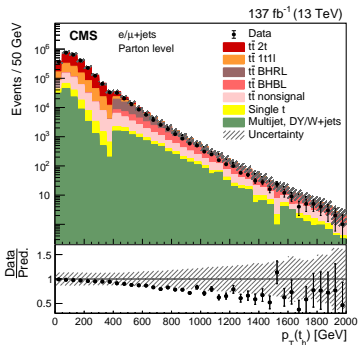
# Differential $t\bar{t}$ cross sections measurements

$e/\mu$ +jets  $137 \text{ fb}^{-1}$ : *Phys. Rev. D 104, 092013*:

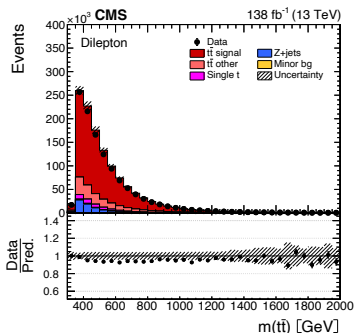
- analysis performed using resolved (3 jets) and boosted (1 fat jet) reconstruction
- cross section extracted fitting all reconstruction categories simultaneously.

dilepton  $138 \text{ fb}^{-1}$ : *Submitted to JHEP*

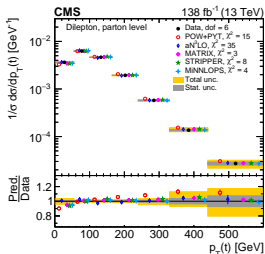
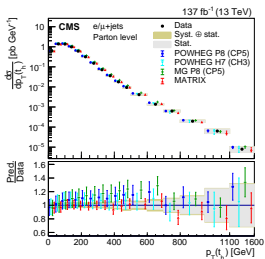
- selection:  $ee, e\mu, \mu\mu$  at least 2 jets, at least 1 b jet.
- find analytic solutions for neutrino momenta; use solution with lowest  $m(t\bar{t})$ . Repeat procedure 100 times varying objects within their resolutions.



BHRL: boosted  $t_h$ , resolved  $t_l$ ; BHBL: boosted  $t_h$  and  $t_l$

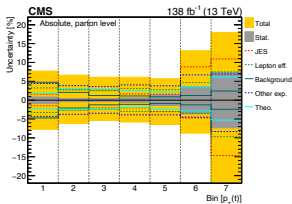
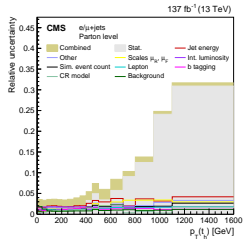


## Results

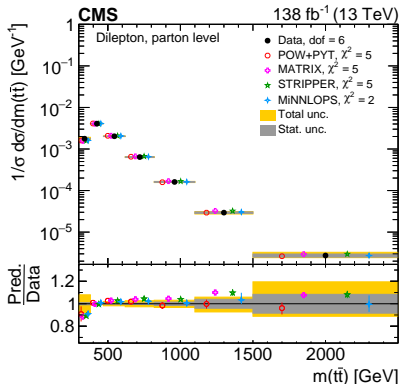
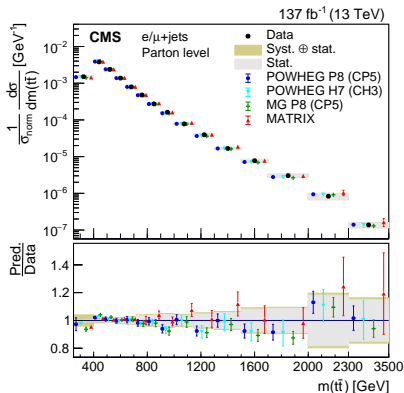


- $p_T$  better described by NNLO calculation.
- trend of harder spectrum in NLO calculations disappears above 600 GeV

## Uncertainties



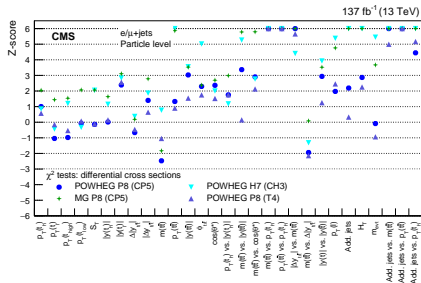
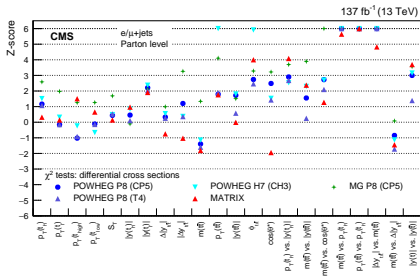
- depending on the phase space region the precision is limited by systematic or statistical uncertainty.
- systematic dominated by experimental uncertainties like jet energy calibration and b-tagging.



- measurements show excess of data at the  $m(t\bar{t})$  production threshold.
- uncertainties in measurements are large in the first bins. Experimental and modelling uncertainties contribute.
- uncertainties in POWHEG+PYTHIA8 are sizable in this bin (This is the only model shown with the full set of variations)

## Comparison of measurements to various predictions using $\chi^2$ -tests

uncertainties in measurements and predictions are taken into account.



Most of the predictions are in good agreement with the measurement—with a few exceptions:

- $m(\bar{t}t)$  vs.  $p_T(t_h)$  and  $p_T(\bar{t}t)$  vs.  $p_T(t_h)$  shows largest disagreements. *but theory uncertainties might be underestimated using fully correlated scale variations*
- at particle level additional jets vs. kinematic observable are not well described. *depends strongly on PS tuning*

Cross section measurements are used:  $m_t$  and  $\alpha_s$  extraction, PDF fits, EFT interpretation ...

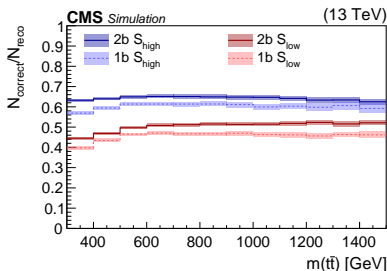
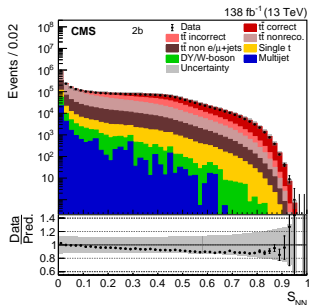
# Extraction of $t\bar{t}$ polarization and spin correlation in $e/\mu$ +jets events

138 fb<sup>-1</sup>, 13 TeV, *submitted Phys. Rev. D*

- in the helicity-frame the differential cross section of particles from  $t\bar{t}$  decays can be parameterized by the polarization vector  $\mathbf{P}$  and the spin correlation matrix  $\mathbf{C}$ :

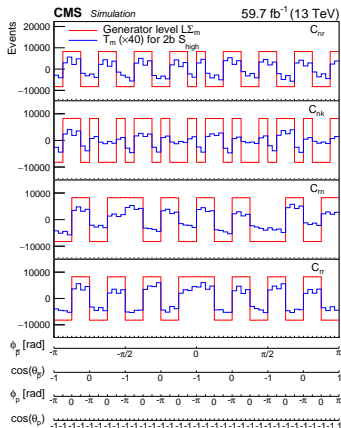
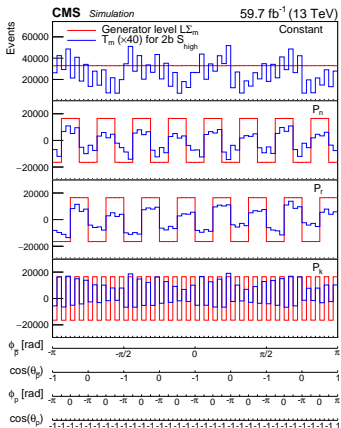
$$\frac{d^4\sigma}{d\Omega d\bar{\Omega}} \propto 1 + \kappa \mathbf{P} \cdot \boldsymbol{\Omega} + \bar{\kappa} \bar{\mathbf{P}} \cdot \bar{\boldsymbol{\Omega}} + \kappa \bar{\kappa} \boldsymbol{\Omega} \cdot \mathbf{C} \bar{\boldsymbol{\Omega}}$$

- together with an overall normalization factor there are 16 parameters to determine
- spin analyzing powers  $\kappa$  depend on the decay particle of the top quark used in the analysis. Best sensitivity ( $\kappa = 1$ ) for charged lepton and down-type quarks from W decays.
- $e/\mu$ +jets final-state: easy reconstruction of top quark momenta, high branching fraction, but challenging to identify the down-type quarks.
- use ML for identification of top decay products based on kinematic and flavor-tagging information (half of the time there is a c-jet in the W decay)



## Extraction method

According to the cross section formula each coefficient is proportional to a function depending on the angles of the two decay products (2 bins in  $\cos(\theta_{p/\bar{p}})$  and 4 bins in  $\phi_{p/\bar{p}}$ ):



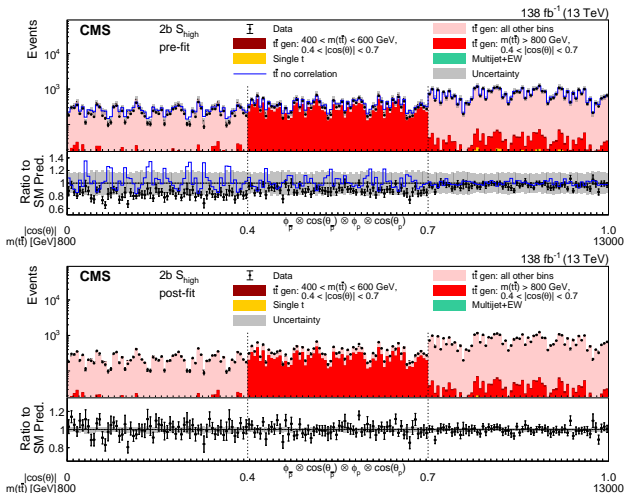
The blue lines show how the detector affects the theoretical shapes (red) due to acceptance, resolution, efficiencies ...

→ Fit linear combination of the detector-level templates to data.



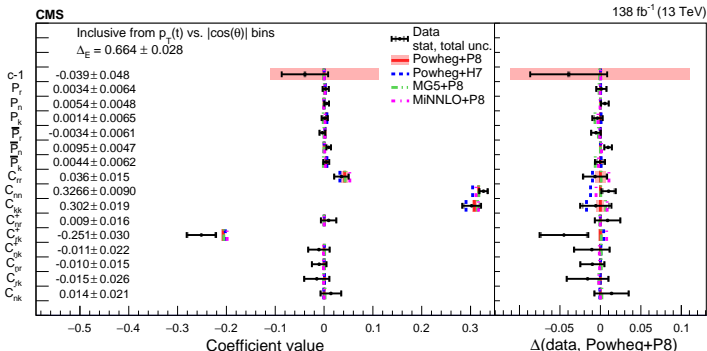
Using the SM  $t\bar{t}$  simulation to construct the templates can result into a bias in the measured coefficients.

→ avoided by fitting in bins of  $t\bar{t}$  distributions:  $m(t\bar{t})$  vs  $\cos(\theta_t)$  or  $p_T(t)$  vs  $\cos(\theta_t)$ :



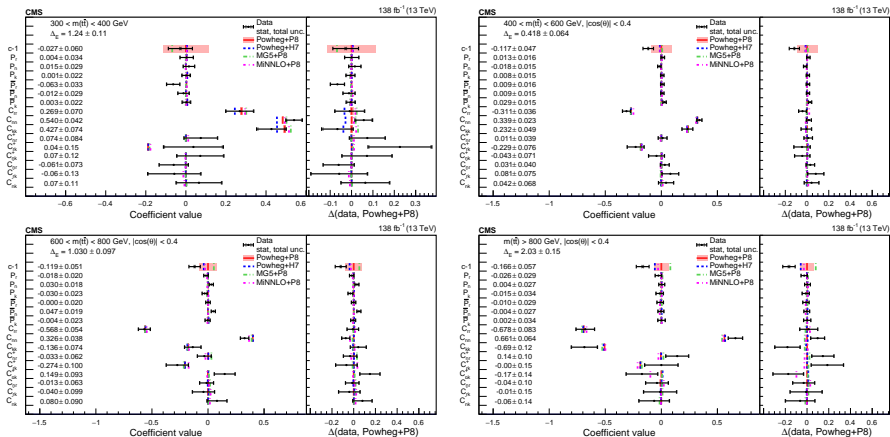
## Inclusive results

From the combination of bins, the inclusive polarization and spin correlation are obtained:



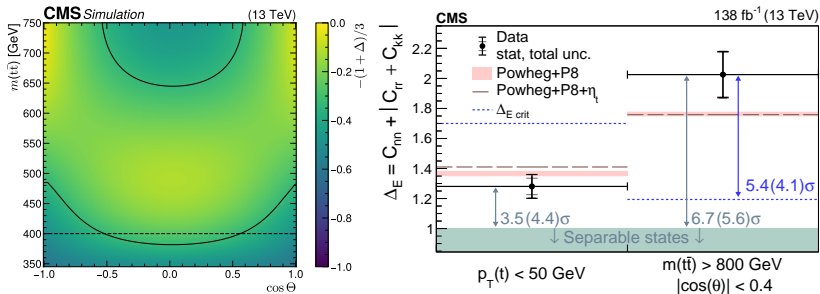
These are in good agreement with the SM expectations; reduction of of uncertainties by about a factor of two with respect to previous measurement (dilepton, with  $36 \text{ fb}^{-1}$ , [Phys. Rev. D 100 \(2019\) 072002](#))

# Differential Results



- the diagonal elements are changing for different  $m(\bar{t}t)$  and  $\cos(\theta_t)$  regions
- statistical uncertainties dominant in most bins  $\rightarrow$  room for improvement with more data

## Quantum Entanglement



- at the threshold and at high  $m(t\bar{t})$  with low  $|\cos(\theta_t)|$   $t\bar{t}$  is expected to be produced in entangled quantum states

A criterion for entanglement (based on Peres–Horodecki):  $\Delta E = C_{nn} + |C_{rr} + C_{kk}| > 1$

First observation of the signature of an entangled quantum state at high  $m(t\bar{t})$ .

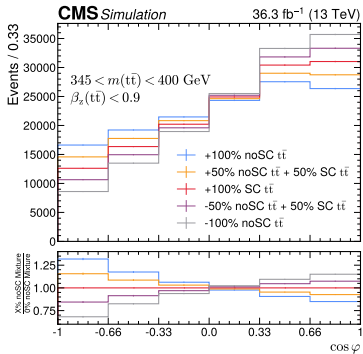
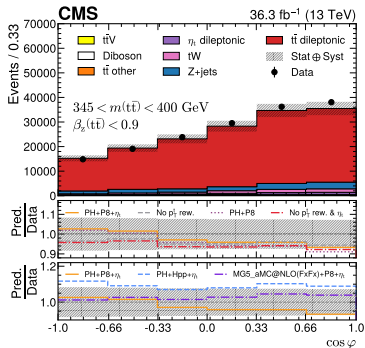
# Entanglement near the threshold in the dilepton final-state

$36 \text{ fb}^{-1}$ , 13 TeV, *accepted by ROPP*

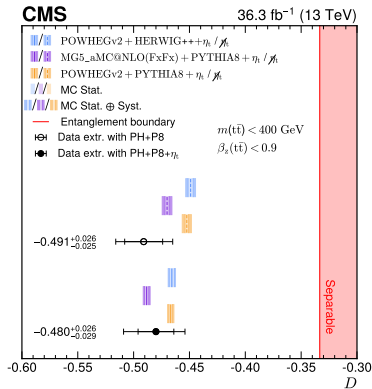
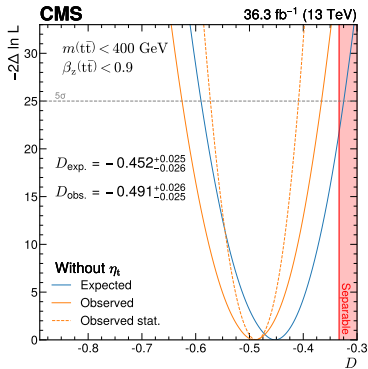
At the  $t\bar{t}$  production threshold, where all diagonal elements of  $C$  are positive  $D = -\frac{1}{3}\Delta E$

$$\frac{d\sigma}{d\cos(\phi)} \propto 1 - D \cos(\phi)$$

This allows for the extraction of the entanglement sensitive observable using the single differential distribution of the opening angle between the two leptons in the helicity-frame.



## Results



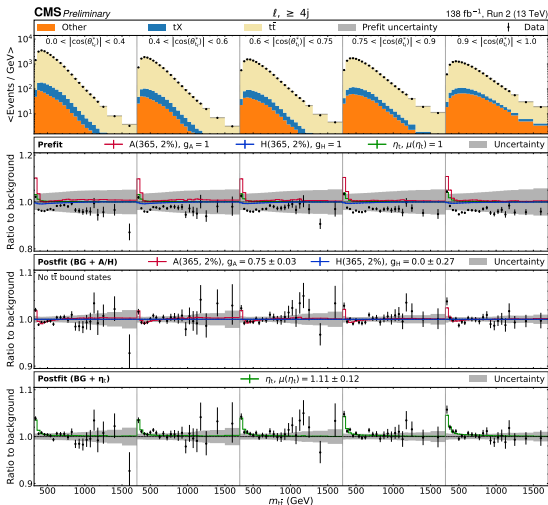
- observation of signature of entanglement with high significance  $D < 1/3$
- uncertainties in the measurement do not allow for a separation between SM hypotheses with and without toponium. (Simulated as pseudo scalar particle with mass of 343 GeV and a production cross section of 6.4 pb.)

# Search for scalar- and pseudo-scalar Higgs decaying into $t\bar{t}$

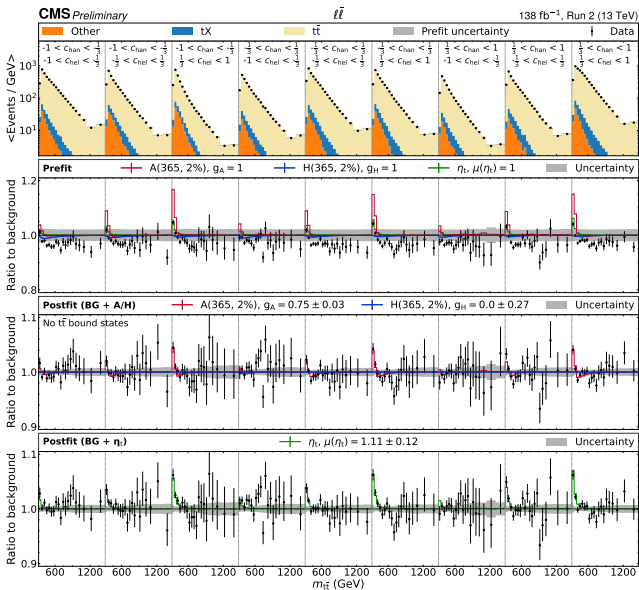
$138 \text{ fb}^{-1}$ , 13 TeV, [HIG-22-013](#)

A search for heavy scalar- and pseudo-scalar Higgs is performed in the  $e/\mu$ +jets and dilepton final-states

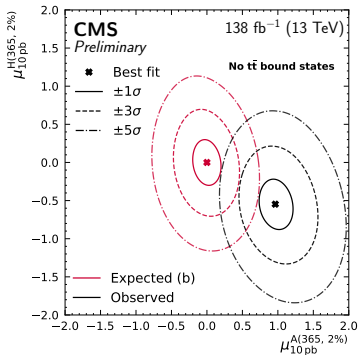
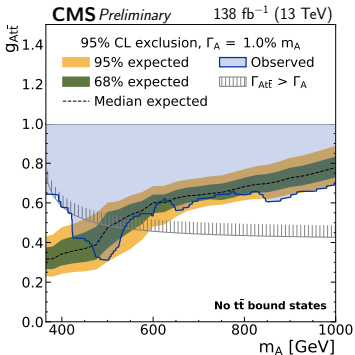
- $e/\mu$ +jets channel uses the scattering angle  $\cos(\theta_t)$  to separate based on the spin



- dilepton channel uses  $c_{\text{hel}}$  (same as  $\cos(\phi)$ , angle between two charged leptons) and  $c_{\text{han}}$  as search variables. Can separate scalar and pseudo scalar states





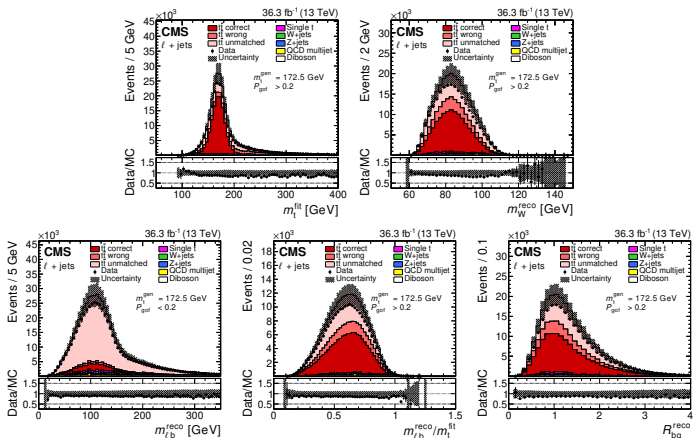


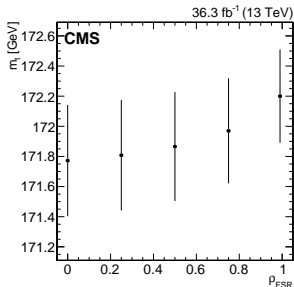
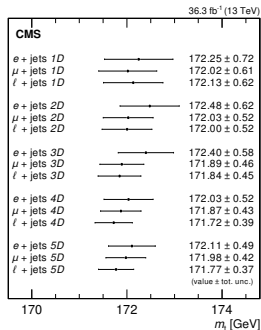
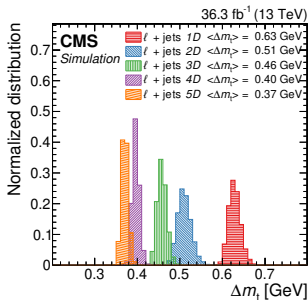
- both channels observe significant excess at the  $t\bar{t}$  production threshold
- data prefer a pseudo scalar contribution for the excess (using the same production cross section for both, tested here with 365 GeV).
- fitted cross section for simple toponium model: 7.1 pb with 11% uncertainty.

# Direct measurement of $m_t$ (MC parameter) in $e/\mu$ +jets events

$36 \text{ fb}^{-1}$ , 13 TeV, *Eur. Phys. J. C* 83 (2023) 963

- select events with  $e/\mu$  and  $\geq 4$  jets
- perform kinematic fitting with constraints of two equal top quark masses and W mass
- goodness of fit also used to determine best parton-jet assignment (47% correct)
- up to 4 distributions + one control region used to extract  $m_t$





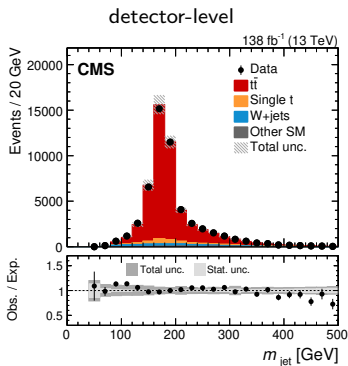
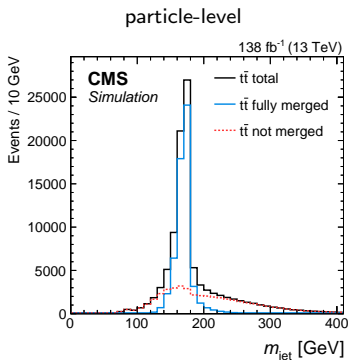
- best fitted value  $m_t = 171.77 \pm 0.37$  GeV
- leading uncertainty is final-state PS scales 0.21 GeV *in contrast to previous measurements uncorrelated scales for different branchings ( $g \rightarrow q\bar{q}$ ,  $q \rightarrow gq \dots$ ) used*
- modelling very important for this measurement

# $m_t$ measurement from boosted hadronically decaying top quarks in $e/\mu$ +jets events

$138 \text{ fb}^{-1}$ , 13 TeV, *Eur. Phys. J. C* 83 (2023) 560

Measure  $m_t$  from unfolded particle-level jet mass

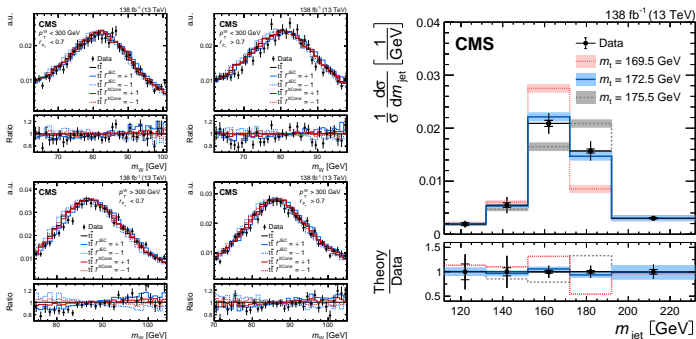
- use X Cone jet algorithm ( $r = 1.2$ ) to find 2 jets: the boosted hadronically decay products ; the lepton and b-jet from the leptonically decay
- use X Cone ( $r = 0.4$ ) to identify the three subjects (combined  $p_T > 400 \text{ GeV}$ , each subject  $p_T > 30 \text{ GeV}$ )



- after excluding the b-subjet the W mass of the remaining two jets is used for the calibration of the jet energy
- from the unfolded jet mass:

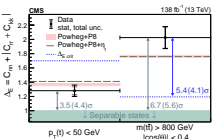
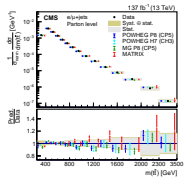
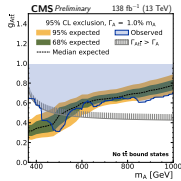
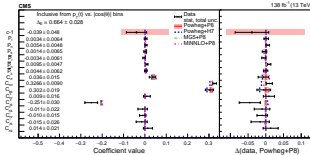
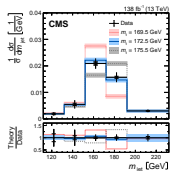
$$m_t = 173.06 \pm 0.84 \text{ GeV}$$

with jet energy and mass calibration being the largest uncertainties.



This method using boosted top quarks provides complementary measurement compared to measurements using low  $p_T$  top quark closer to the threshold, in particular with respect to theoretical uncertainties.

# Conclusion



## Measurement of (multi) differential cross sections:

- performed in many channels; resolved and boosted reconstructions
- used to determine:  $m_t$ , PDFs, EFT limits, MC tunes

## Spin correlations:

- first measurement of spin correlations in various regions of the  $t\bar{t}$  phase space
- first characterization of  $t\bar{t}$  quantum state as entangled

## Significant pseudo-scalar-like excess at the $t\bar{t}$ production threshold

## Top quark mass:

- new precise and complementary measurements with boosted top quarks
- improved techniques leveraging in-situ constraints for higher precision

